

# Phase diagram of aggregation of oppositely charged colloids in salty water

R. Zhang and B. I. Shklovskii

*Theoretical Physics Institute, University of Minnesota, Minneapolis, Minnesota 55455*

(Dated: May 22, 2019)

Aggregation of two oppositely charged colloids in salty water is studied. We focus on strongly asymmetric systems in which the charge and size of one colloid is much larger than the other and concentrate on the role of Coulomb interaction. In the solution, each large colloid (macroion) attracts certain number of oppositely charged small colloids (Z-ion) to form a complex. If the concentration ratio of the two colloids is such that complexes are not strongly charged, they condense in a macroscopic aggregate. As a result, the phase diagram in a plane of concentrations of two colloids consists of an aggregation domain sandwiched between two domains of stable solutions of complexes. The aggregation domain consists of a central part of total aggregation and two wings corresponding to partial aggregation. A quantitative theory of the phase diagram in the presence of monovalent salt is developed. It is shown that as the Debye-Hückel screening radius  $r_s$  decreases, the aggregation domain grows, but the relative size of the partial aggregation domains becomes much smaller. As an important application of the theory, we consider solutions of long double-helix DNA with strongly charged positive spheres (artificial chromatin). We also consider implications of our theory to vitro experiments with the natural chromatin. Finally, the effect of different shapes of macroions to the phase diagram is discussed.

## I. INTRODUCTION

Aggregation or self-assembly of oppositely charged colloids is a general phenomenon in biology, pharmacology, and chemical engineering. The most famous biological example is the chromatin made of long negatively charged double-helix DNA and positively charged histone octamers<sup>1</sup>. Due to Coulomb interaction, DNA winds around many octamers to form a beads-on-a-string structure, also called 10 nm fiber (see Fig. 1 for an illustration). This 10 nm fiber may self-assemble into a 30 nm fiber which is the major building material of a chromosome. The formation of 30 nm fiber strongly depends on the concentration of salts in the solution. This means that Coulomb interaction plays a crucial role<sup>2</sup>. The best known pharmacological example is the problem of gene therapy. In this case, a negatively charged DNA helix should penetrate through negatively charged membrane. To do this, DNA must be neutralized or overcharged by complexation with positive polyelectrolytes or colloids. At the same time aggregation of these complexes can be useful or should be avoided<sup>3,4,5,6,7,8,9</sup>. Industrial examples include using cationic polyelectrolyte as coagulants for paper manufacturing, mineral separation, and the aggregation induced removal of particulate matter from the aqueous phase in water and waste water treatment processes<sup>10</sup>. All these examples show that the aggregation induced by electrostatic Coulomb interaction between oppositely charged colloids is a very general phenomenon. It is therefore interesting to construct a general physical theory to explain all these phenomena in the same manner.

In this paper, we consider the equilibrium state of two kinds of oppositely charged colloids in salty water and construct the phase diagram of the system. Without losing generality, we concentrate on a system which contains negatively charged macroions with charge  $-Q$  and posi-

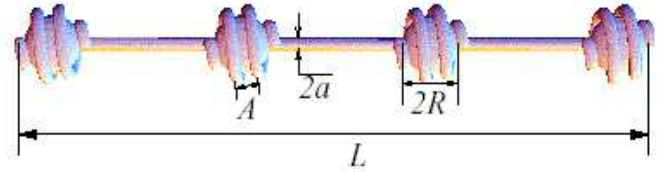


FIG. 1: A beads-on-a-string structure of the complex of a long polymer macroion with spherical Z-ions. Spheres strongly repel each other to form almost periodic structure. The turns of the polymer on the surface of Z-ions also repel each other to form an almost equidistant coil.

tively charged multivalent ions with charge  $Ze$  (which we call Z-ions as in Ref. 11) in a water solution,  $e$  being the proton charge. There is also a large amount of monovalent salt in the solution. Macroions can be big spheres (big colloid particles), rigid cylinders (short DNA) or long semi-flexible polymers (long DNA). Z-ions can be small spheres (nucleosome core particles, micelles or dendrimers) or short polymers (polyamines). Most of such systems are strongly asymmetric in the sense that the size and charge of the macroion are much larger than those of the Z-ion (Figs. 1, 2, 3). We define the number of Z-ions needed to neutralize one macroion as  $N_i = Q/Ze$  (the subscript  $i$  denoting “isoelectric”), and focus on systems with  $N_i \gg 1$ . We do not consider cases when the size of macroion is bigger than that of Z-ion but the charge is smaller or vice versa.

In a previous paper<sup>11</sup> the same equilibrium state problem was considered for long semi-flexible polymers (DNA) as macroions and rigid spheres as Z-ions (Fig. 1) which we call artificial chromatin. The phase diagram of reentrant condensation in the plane of two concentrations was obtained (Fig. 4a). It can be seen from the phase diagram that the equilibrium state of the system

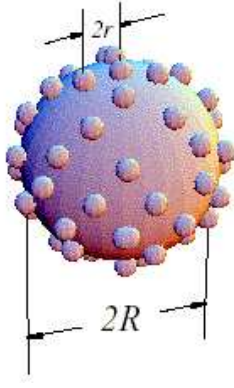


FIG. 2: A spherical negative macroion with spherical positive Z-ions condensing on it. Z-ions strongly repel each other and form 2D Wigner-crystal-like liquid on the surface of the macroion.

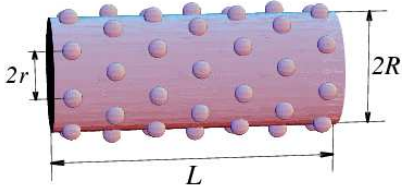


FIG. 3: A negative cylindrical macroion with positive spherical Z-ions condensing on it. Z-ions form 2D Wigner-crystal-like liquid on the surface of the macroion.

is determined by the ratio of the Z-ion concentration,  $s$ , to the macroion concentration,  $p$  (notations  $s$  and  $p$  are introduced as abbreviation for “sphere” and “polymer” in the present case). At  $s/p < N_i$ , the number of Z-ions is not large enough to neutralize macroions. Each polymer macroion winds around a number of spherical Z-ions and forms a periodic necklace-like structure. The net charge of this necklace is negative. At  $s/p > N_i$ , Z-ions overcharge a macroion and form a necklace structure with positive net charge. Far enough from  $s/p = N_i$ , the Coulomb repulsion between necklaces is huge and the aggregation of them is impossible. At  $s/p \sim N_i$ , the necklace is almost neutral and the aggregate is formed due to the short range attraction between spheres covered by the polymer coil (see Fig. 5).

It should be emphasized that strong correlations play a crucial role in this picture. First, spherical Z-ions in the necklace repel each other to form a 1D liquid with almost periodic structure as Wigner crystal (WC) in short range. This leads to a negative correlation energy in addition to the mean field Coulomb energy of the Z-ion. This additional energy related to  $Ze$  plays the role of a voltage overcharging necklaces (making them positive) at  $s/p > N_i$ . Second, the polymer turns wound around a spherical Z-ion repel each other and result in an almost equidistant

coil. At  $s/p - N_i \ll N_i$ , the charges of necklaces are so small that short range correlation of two coils is able to condense them (Fig. 5).

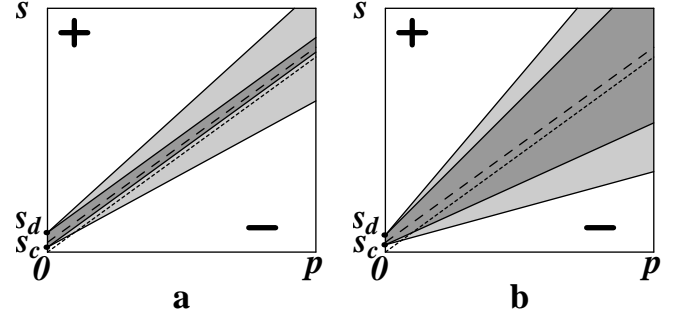


FIG. 4: Phase diagrams of the artificial chromatin system. **a**: without monovalent salt. **b**: with monovalent salt. (Spherical and cylindrical macroion systems have similar phase diagrams with a much larger  $s_d$ .)  $p$  is the concentration of macroions,  $s$  is the concentration of Z-ions. Plus and minus are the signs of the charge of free macroion-Z-ions complexes. The dark gray region is the domain of total aggregation of macroions, while the light gray region is the domain of their partial aggregation. The white region is the domain of the dispersed state of free complexes.  $s_c$  and  $s_d$  are concentrations of Z-ions at the boundary of the aggregation domain when  $p \rightarrow 0$ . At the dotted line the absolute value of total charge of macroions equals to that of Z-ions. At the dashed line a free macroion adsorbs exactly  $N_i$  Z-ions and is neutral.

An important feature of the phase diagram in the absence of monovalent salt (Fig. 4a) is the wide domain, where aggregation of macroion-Z-ions complexes is only partial. The reason for partial aggregation is that a macroscopic aggregate should be neutral. Since almost all Z-ions are consumed by complexes, this neutrality is reached by redistribution of Z-ions between complexes. For example, at  $s/p < N_i$ , free complexes yield Z-ions to those aggregated to make them neutral. As a result free complexes become even more negative, repel each other and stay free.

In this paper we generalize results of Ref. 11 by considering the screening effect of monovalent salt. The screening cuts off the Coulomb interaction at the Debye-Hückel screening radius  $r_s$ . If  $r_s$  is smaller than the size of the macroion (for example, for spherical macroions), the Coulomb repulsion of two macroion-Z-ions complexes is almost completely screened even when they touch each other. Therefore, the aggregation is possible even if macroion-Z-ions complexes carry a net charge. The phase diagram in the presence of monovalent salt is plotted in Fig. 4b. Comparing with the phase diagram in the absence of monovalent salt (Fig. 4a), we see that as  $r_s$  decreases, the aggregation domain (including both partial and total aggregation domains) grows. The domain of the total aggregation (dark gray region in Fig. 4) also grows so that the slope of its upper (lower) boundary is

larger (smaller) than that of the isoelectric line  $s_i = pN_i$  (dotted line in Fig. 4). At the same time, the relative size of the partial aggregation domain (light gray region in Fig. 4) to the whole aggregation domain decreases, because redistribution of Z-ions becomes less important.

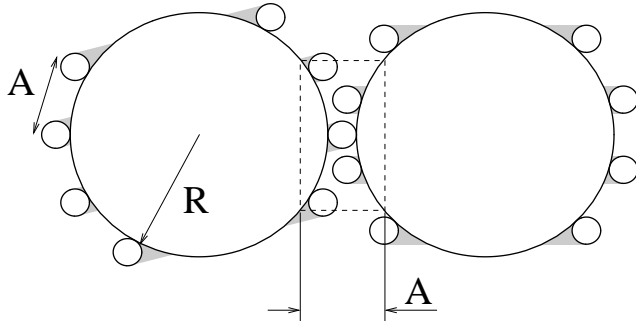


FIG. 5: Cross section through the centers of two touching spherical Z-ions with turns of semi-flexible polymers (gray) wound around them. At the place where two spheres touch each other the density of macroion segment doubles which in turn leads to a gain in the correlation energy.

Two general remarks should be made about the phase diagram. First, as seen from Fig. 4a, the phase diagram is asymmetric with respect of the isoelectric line  $s_i = pN_i$  (dotted line) in the sense that we have total aggregation (dark gray) at the upper side of it but only partial aggregation (light gray) at the lower side. This is because by definition, we always focus on total or partial aggregation of *macroions*. Below the isoelectric line, the number of Z-ions is not enough to neutralize all macroions so that total aggregation of macroions is impossible (remember the aggregate must be neutral without monovalent salt). Second, as we already pointed out, as  $r_s$  decreases, the aggregation domain in Fig. 4b grows. But it does not go for ever. When the decreasing  $r_s$  passes through the distance between Z-ions on the surface of a macroion (e.g., for spherical macroions), the width of the aggregation domain goes through maximum and then vanishes at some critical  $r_s$ . At this critical  $r_s$ , the short range correlation is also screened out and the aggregate completely dissolves.

The phase diagram (Fig. 4b) is important to qualitatively understand the behavior of natural chromatin in vitro when DNA is cut into many pieces. In this case the role of spheres in our artificial chromatin model is played by strongly positively charged histone octamers. First, in the presence of monovalent salt, the net charge of the aggregate (the total charge of DNA and histone octamers) need not to be neutral. This explains why each nucleosome and the whole chromatin are negatively charged but can still aggregate into 30 nm fiber and higher order structures. Second, the relative size of the partial aggregation domain is very small in the presence of monovalent

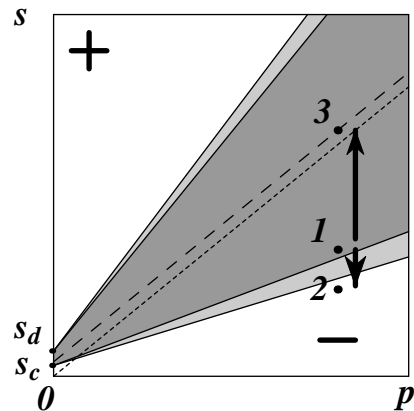


FIG. 6: The chromatin regulation and compaction.  $s$  is the concentration of histones,  $p$  is the concentration of DNA. All other labels have the same meaning as in Fig. 4. Before acetylation of histones, the chromatin solution is at the point 1. After acetylation of histones, it moves to the point 2 (downward arrow). On the other hand, addition of protamines during spermatogenesis compacts chromatin into the most condensed state 3 (upward arrow).

salt. This is important for the regulation of natural chromatin. It is known<sup>1</sup> that chromatin can switch between two different states. One is the loose state of 10 nm fiber in which gene transcription takes place; the other is the compact state where 10 nm fiber self-aggregates in 30 nm fiber and higher order structures. Transition from the compact state to the loose state is done by acetylation of the core histones which reduces the number of positive charges of histone octamers. Experiments<sup>12</sup> in vitro show that the transition happens when the charge of octamer (about +160e in normal conditions) is reduced by +12e, i.e., only by 8%. Such a sensitive response can be qualitatively understood in our theory as shown in Fig. 6. Initially, the chromatin solution is at point 1 which is in the total aggregation domain and very close to its lower boundary. After acetylation, the charge of octamers is reduced so that effectively the concentration of Z-ions,  $s$ , decreases. Consequently the system goes to point 2 which is outside the aggregation domain. The small partial aggregation domain in this case is crucial for the sensitive response. Third, the phase diagram of Fig. 6 can also help to understand what happens when the relatively compacted state 1 is compacted further during spermatogenesis. This happens due to addition of certain strongly positive charged proteins, protamines<sup>1</sup>. As a result, the chromatin solution moves up in the phase diagram supposedly to the most condensed neutral state 3 at the dashed line of Fig. 6.

At the end of the paper, we consider the effect of the shape and flexibility of macroions on the phase diagram. Specifically, we construct the phase diagrams for systems shown in Figs. 2 and 3. These two systems are different from the artificial chromatin system mostly in the nature of the short range correlation due to aggregation.

As a result, the values of  $s_d$  (see Fig. 4) are very different for different systems. In the artificial chromatin case (Fig. 1),  $s_d$  is an exponentially small number and the aggregation domain at small  $p$  is very small. In the spherical macroion (Fig. 2) and cylindrical macroion (Fig. 3) cases,  $s_d$  is not exponentially small and the aggregation domain is significantly wider at small  $p$ .

This paper is organized as follows. In Sec. II, the general theory with the screening effect of monovalent salt is discussed. In Sec. III, we deal with the artificial chromatin (Fig. 1). In Sec. IV, systems shown in Figs. 2 and 3 are considered. In Sec. V, we comment on the role of kinetics.

## II. AGGREGATION IN THE PRESENCE OF MONOVALENT SALT

In this section we discuss the general theory of the phase diagram in the presence of monovalent salt using the simplest system shown in Fig. 2. We show below that screening enlarges the aggregation domain by opening its boundaries in the phase diagram. This effect becomes strong only when  $r_s < R$ ,  $R$  being the size of the macroion. On the other hand, if  $r_s$  is too small,  $r_s \ll r$ , short range correlations are also screened out and the aggregation is not possible any more. Here  $r$  is the half average distance between Z-ions on the macroion surface or the radius of the Wigner-Seitz cell, when a macroion is neutralized by Z-ions (see Fig. 2). Therefore the interesting regime we want to study is  $r \ll r_s \ll R$ .

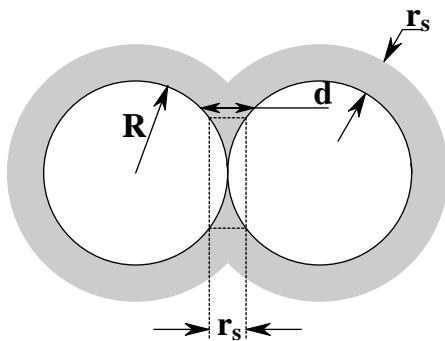


FIG. 7: The cross section of the two spherical macroions. Z-ions adsorbed on them are not shown. The width of the gray region is the effective range of the Coulomb interaction in the presence of monovalent salt. The neutral region is showed in the rectangle of dashed lines.

As discussed in Sec. I, there are two low free energy states in the system. In the first state, each macroion attracts certain number of Z-ions to form a free macroion-Z-ions complex in the bulk. In the second state, macroion-Z-ions complexes are condensed into an aggregate. The aggregate can be formed because of the short range correlation energy gain. Similar to Fig. 5, in the system of spherical macroions, when two spherical macroions touch

each other, the surface density of Z-ions in the contact region is doubled, and the correlational energy is gained. When the screening effect of monovalent salt is negligible, each macroion can only carry  $N_i$  Z-ions in the aggregate, i.e., the aggregate is almost neutral. This is because if macroion-Z-ions complexes were charged, the Coulomb potential of the aggregate would increase with its size and become too large to continue aggregation. On the other hand, in the presence of strong screening by monovalent salt, the aggregate of macroion-Z-ions complexes does not need to be neutral, only the touching region shown in Fig. 7 should be neutral. Looking at Fig. 7, we see that when the local distance between the two touching surfaces,  $d$ , is larger than the order of  $r_s$ , the Coulomb interaction between two surfaces is exponentially small and can be forgotten. If we define a disk-like region as the part of the macroion surface with  $d \leq r_s$ , it is easy to see that neutralization upon aggregating happens only in this region. The rest of the surface is the same as that of free macroions.

We now argue why this disk-like region should be almost neutral. In Fig. 7, at distance  $d \ll r_s$ , the charge distribution on the surface of the two spheres is the same as on two contacting metallic spheres. Then it is known that the surface charge density goes to zero when we move to the point of contact because the surface becomes more and more “concave”. Approximately, we can say that the whole disk-like region is neutral. Another way to see this point is to consider a simple toy model to estimate the surface charge density near the contact point,  $\sigma'$ , from above. In this model, we make macroions hollow so that water can go inside. Then we can assume that Debye-Hückel screening of each charge by monovalent salt is linear and does not change when macroions approach each other. The potential of any point on the rest of the surface is  $2\pi\sigma r_s$ . While near the contact point, both surfaces contribute and the potential is  $4\pi\sigma' r_s$ . Since the two potential must be equal to each other, we get  $\sigma' = \sigma/2$ . Of course, this toy model is unrealistic. In real systems, water can not penetrate into macroions and the dielectric constant of the macroion is much smaller than water. Consequently, screening by monovalent salt is strongly modified when  $d < r_s$  and  $\sigma'$  is much smaller than  $\sigma/2$ . Therefore we have good reason to use the approximation that the disk-like region is neutral, i.e.,  $\sigma' = 0$ .

Notice that this disk-like region is different from the contact region where the additional correlational energy is gained (see Fig. 5, where the distance  $A$  between two polymer turns corresponds to  $2r$  between two Z-ions in the present case). Since  $r \ll r_s$ , the contact region shown in Fig. 5 is much smaller than the disk-like region in Fig. 7. For clarity, we call the former “contact region”, the latter “neutral region”. Below, we use  $\beta$  for the ratio of the area of all neutral regions to that of the total surface of a macroion. (Notice that each macroion can touch several others and have several neutral regions in the aggregate.) Obviously,  $\beta$  is a monotonically increas-

ing function of  $r_s$  with the maximum value 1. From the definition of  $\beta$ , in the aggregate, the number of Z-ions in the neutral region is  $\beta N_i$ , and the total number of Z-ions on a macroion is  $(1 - \beta)N + \beta N_i$ .

Now we can set up the free energy of the system analytically. Following Ref. 11, the basic idea of the theory is to consider an equilibrium between the two low free energy states in the system. Supposing each free macroion-Z-ions complex carry  $N$  Z-ions, and the fraction of macroion-Z-ions complexes in the aggregate is  $x$ , the free energy per unit volume is

$$\begin{aligned} F(N, x; s, p) = & (1 - x)p \left[ \frac{Q^{*2}}{2C} + NE(N) \right] \\ & + xp \left[ (1 - \beta) \frac{Q^{*2}}{2C} + (1 - \beta)NE(N) + \beta N_i E(N_i) + \epsilon \right] \\ & + k_B T [s - xp((1 - \beta)N + \beta N_i) - (1 - x)pN] \\ & \times \ln \frac{[s - xp((1 - \beta)N + \beta N_i) - (1 - x)pN]v_0}{e}. \end{aligned} \quad (1)$$

The first term is the free energy density of free macroion-Z-ions complexes, where  $Q^*$  and  $C$  are the net charge and capacitance of a complex,  $E(N) < 0$  is the correlation energy gain per Z-ion in the complex. The second term is the free energy density of the aggregate.  $\epsilon < 0$  is the additional correlation energy gain per macroion in the aggregate<sup>13</sup>. The third term is the free energy density of free Z-ions due to their entropy, where  $v_0$  is the normalizing volume. The entropy of macroions is ignored because of their much smaller concentration. Minimizing this free energy with respect to  $x$  and  $N$ , we get

$$\mu_c + \frac{ZeQ^*}{C} = k_B T \ln[(s - (1 - x)pN - xp((1 - \beta)N + \beta N_i))v_0], \quad (2)$$

$$\epsilon - \beta \frac{Q^{*2}}{2C} = \beta(N - N_i) \{ \mu_c - k_B T \ln[(s - (1 - x)pN - xp((1 - \beta)N + \beta N_i))v_0] \}, \quad (3)$$

where  $\mu_c(N) = \partial(NE(N))/\partial N < 0$  is the part of the chemical potential of Z-ions related to correlation and it has been assumed in Eqs. (2) and (3) that  $\mu_c(N) \simeq \mu_c(N_i) \equiv \mu_c$  (this will be confirmed later). Solving Eqs. (2) and (3), we get

$$N_{c,d} = N_i \left( 1 \mp \sqrt{\frac{|\epsilon|}{\beta(r_s)} \frac{2C(r_s)}{Q^2}} \right), \quad (4)$$

where  $N_{c,d}$  are the numbers of Z-ions carried by one free macroion in partial aggregation domains. Here and below, the upper (lower) sign of plus and minus in the formula always corresponds to the first (second) subscript of the symbol. Plugging Eq. (4) back to Eq. (2), we get

$$s_{c,d}(p) = s_{c,d} + (1 - x)pN_{c,d} + xp[(1 - \beta)N_{c,d} + \beta N_i], \quad (5)$$

where

$$s_{c,d} = \frac{1}{v_0} \exp \left[ \frac{1}{k_B T} \left( \mp \sqrt{\frac{|\epsilon|}{\beta(r_s)} \frac{2Z^2 e^2}{C(r_s)}} - |\mu_c| \right) \right] \quad (6)$$

are the concentrations of Z-ions at the aggregation boundaries when  $p$  is very small (see Fig. 4). The two solutions  $N_{c,d}$  and  $s_{c,d}$  mean that we have two partial aggregation domains. Taking  $x = 0$  and  $x = 1$  in Eq. (5), we get two outer boundaries

$$s_{c,d}(p; x = 0) = s_{c,d} + pN_{c,d}, \quad (7)$$

and two inner boundaries

$$s_{c,d}(p; x = 1) = s_{c,d} + p[(1 - \beta(r_s))N_{c,d} + \beta(r_s)N_i] \quad (8)$$

of partial aggregation domains. The corresponding phase diagram is shown in Fig. 4b. The outer boundaries are also the boundaries of the whole aggregation domain (including partial and total aggregation domains), at which all free macroion-Z-ions complexes are stable ( $x = 0$ ). The inner boundaries are also the boundaries of the total aggregation domain at which there is no free macroion-Z-ions complex ( $x = 1$ ). When  $s$  increases from zero, first the aggregate forms, then it dissolves. Thus we arrive at a phase diagram of reentrant condensation. According to Eq. (7), the slopes,  $ds/dp$ , of the outer boundaries are  $N_{c,d}$ , which are the numbers of Z-ions on one free macroion (see Eq. (1)). Since  $N_{c,d}$  are solutions for  $N$  which are valid in the whole partial aggregation domain, the number of Z-ions on one free macroion is fixed in the partial aggregation domain. According to Eq. (8), the slopes of the inner boundaries are  $(1 - \beta)N_{c,d} + \beta N_i$ , which are the number of Z-ions on one macroion in the aggregate (see Eq. (1)). The dashed line on Fig. 4b corresponds to solutions with neutral macroion-Z-ions complexes and can be calculated from Eq. (2). Taking  $N = N_i$  in this equation, We get

$$s(p) = \frac{1}{v_0} \exp \left( -\frac{|\mu_c|}{k_B T} \right) + pN_i. \quad (9)$$

This line has the same slope as the isoelectric line  $s_i = pN_i$  (dotted line in Fig. 4) but different intercept. This is because there are always a small fraction of Z-ions being free in the solution.

There are four input parameters  $\mu_c$ ,  $\epsilon$ ,  $C$  and  $\beta$  in the theory. Their values depend on the screening radius  $r_s$ , and the shape and flexibility of the macroions and Z-ions. In later sections, we calculate them for certain specific systems. Remember that the assumption  $\mu_c(N) \simeq \mu_c(N_i) \equiv \mu_c$  is used in the derivation. This assumption is valid only if the aggregation happens around neutrality, i.e.,  $N_{c,d}$  are close to  $N_i$ . Consequently, according to Eq. (4), we must have

$$|\epsilon| \ll \beta(r_s) \frac{Q^2}{2C(r_s)}. \quad (10)$$

In following sections, we show that this condition is always satisfied as far as  $r_s \gg r$ .

If we let  $\beta = 1$ , the whole surface of a macroion in the aggregate is neutral, all formulae above reproduce the corresponding results in the case when the screening

effect of monovalent salt can be ignored<sup>11</sup>. The corresponding phase diagram is shown in Fig. 4a. In this case, the boundaries of the total aggregation domain given by Eq. (8) are simply reduced to

$$s_{c,d}(p; x=1) = s_{c,d} + pN_i. \quad (11)$$

Let us discuss the change of the phase diagram when we reduce  $r_s$  and go from Fig. 4a to Fig. 4b. To do this, it is convenient to define the effective size of an aggregation domain as the absolute value of difference of slopes,  $ds/dp$ , of its two boundaries. We also notice that as  $r_s$  decreases,  $\beta(r_s)$  decreases,  $C(r_s)$  increases, while  $\epsilon$  is fixed (this will be shown in later section). Then according to Eq. (4),  $N_d$  increases and  $N_c$  decreases. Thus according to Eq. (7), the size of the whole aggregation domain (including partial and total aggregation domains) is given by  $N_d - N_c$ , and grows with decreasing  $r_s$ . According to Eq. (8), the size of the total aggregation domain is given by  $(1 - \beta)(N_d - N_c)$ , also grows with decreasing  $r_s$ . Consequently, the relative size of the two partial aggregation domains to the whole aggregation domain (including partial and total aggregation domains),  $\beta(N_d - N_c)/(N_d - N_c) = \beta$ , decreases with decreasing  $r_s$ .

### III. ARTIFICIAL CHROMATIN

In this section, we discuss the artificial chromatin system in which macroions are long semi-flexible polymers and Z-ions are hard spheres with radius  $R$  (Fig. 1). The phase diagram of this system has already been discussed in detail in Ref. 11 under the assumption that the aggregate is always neutral. In the case when the screening effect of monovalent salt can be ignored, i.e.,  $r_s \gg R$ , this assumption is correct. But when  $r_s \ll R$ , as we see above, the screening effect is so important that there is no justification for the neutrality of the aggregate. Therefore, our main task in this section is to give the correct theory and results with screening. Specifically, we consider the case in which  $A \ll r_s \ll R$ ,  $A$  being the distance between two polymer turns on the surface of spheres in the case when polymer segments exactly neutralize the sphere (see Fig. 1). Since  $\eta/A \simeq Ze/R^2$ , the requirement  $A \ll R$  is equivalent to  $R\eta \ll Ze$ , i.e., many turns of polymer segments are needed to neutralize one sphere.

First, we give the results with  $r_s \gg R$  following directly from Ref. 11. In this case, each macroion-Z-ions complex carries  $N_i$  Z-ions in the aggregate. Correspondingly,  $\beta = 1$ . The correlation chemical potential  $\mu_c$  is essentially the self-energy of a bare free sphere in the solution which is almost totally eliminated in the complex. Therefore

$$\mu_c = -\frac{Z^2 e^2}{2DR}, \quad (12)$$

where  $D$  is the dielectric constant in water solution. To calculate  $\epsilon$ , we first notice that the correlation energy per

unit length of the polymer is just the interaction energy of the polymer turn with its stripe of background (sphere) positive charge. Thus, it is  $-\eta^2 \ln(R/A)/D$ . Correspondingly, when the density doubles,  $A$  is halved, the gain in correlation energy per unit length is  $-\alpha\eta^2/D$ , where  $\alpha = \ln 2$  as a rough estimation. The radius of the contact region in which one sphere touch another sphere,  $W$ , can be estimated as following (see Fig. 5). At the distance  $W$  from the contact point, the surfaces of two spheres diverge from each other at the distance of the order of  $A/2$ . Beyond  $W$ , the interaction between 1D Wigner crystals of two macroions is exponentially weak. A simple geometrical consideration gives  $W \simeq \sqrt{RA/2}$ <sup>14</sup>. And the polymer length in this region is  $\pi W^2 \eta/A = \pi R \eta/2$ . Since each aggregated complex carries  $N_i$  Z-ions and has  $b$  nearest neighbors, we have

$$\epsilon = -\frac{\pi b \alpha}{2} \frac{R \eta^2}{D} N_i, \quad (13)$$

where  $b = 6$  if the maximum packing number is achieved. The capacitance

$$C = \frac{DL}{2 \ln(r_s/R)} = \frac{DR N_i}{\ln(r_s/R)}, \quad (14)$$

where we have used  $L \simeq 2R N_i$ , because near neutrality, each polymer absorbs about  $N_i$  spheres and all spheres in the macroion-Z-ions complex are densely packed. Using Eqs. (4) and (6), we have

$$\begin{aligned} N_{c,d} &= N_i \left( 1 \mp \sqrt{\frac{\pi b \alpha}{\ln(r_s/R)} \frac{R \eta}{Ze}} \right), \\ s_{c,d} &= \frac{1}{v_0} \exp \left[ -\frac{Z^2 e^2}{2k_B T D R} \left( 1 \pm 2 \sqrt{\pi b \alpha \ln \frac{r_s}{R} \frac{R \eta}{Ze}} \right) \right]. \end{aligned} \quad (15)$$

This gives a typical phase diagram of reentrant condensation (Fig. 4a).

Now let us consider the case when  $A \ll r_s \ll R$ . As we discussed in Sec. II, with the screening of monovalent salt, the whole aggregate does not need to be neutral, but disk-like regions on spheres where two spheres touch each other must be neutral (see Fig. 7). Similar to the estimation of  $W$ , the radius of this region  $W_s = \sqrt{r_s R}$ . In the present case, the neutral region should be made by the rearrangement of the polymer segments on the surface of spheres. If the polymer is extremely flexible, it can bend easily in the disk-like region. By this bending, the surface density of polymer segments is changed “locally” so that the region can be made neutral and the rest of the surface is untouched. However, if the polymer is only semi-flexible (the persistent length  $l_p$  is such that  $\sqrt{r_s R} \ll l_p \ll R$ ), it is too rigid to neutralize the disk-like region. Then this region can be made neutral only by changing distances between sequential turns of the polymer on the surface of the sphere. For example, for two touching spheres (Fig. 5), the equatorial stripe-like

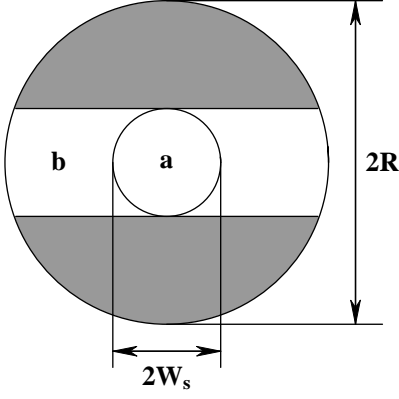


FIG. 8: A 2D view of the surface of a sphere touching the other sphere at the center of the disk-like region **a**. To make **a** neutral, a semi-flexible polymer have to change the density of its turns to make the whole equatorial stripe-like region **b** neutral. The rest of the surface colored in gray is charged.

region shown in Fig. 8 can be made neutral. We focus on the case of the semi-flexible polymer which corresponds to DNA.

When  $A \ll r_s \ll R$ , the correlation chemical potential  $\mu_c$  is still given by the self-energy of a bare free sphere, which is now

$$\mu_c = -\frac{r_s Z^2 e^2}{2DR^2}, \quad (17)$$

and the correlation gain due to aggregation,  $\epsilon$ , is still given by Eq. (13). This is because the contact region where the additional correlational energy is gained is much smaller than the neutral region as discussed in Sec. II. Also since the number of Z-ions in each complex in the aggregate is close to  $N_i$ , in the first order approximation, we can use  $N_i$  as the number of Z-ions in each complexes in  $\epsilon$ . Knowing that the area of the strip-like region is  $4\pi W_s R$  (see Fig. 8), the area ratio  $\beta$  is given by

$$\beta = \frac{4\pi W_s R}{4\pi R^2} = \sqrt{\frac{r_s}{R}}. \quad (18)$$

Finally, the capacitance is now

$$C = \frac{DR}{2r_s} = \frac{DR^2}{r_s} N_i. \quad (19)$$

Using Eqs. (4) and (6), the specifications of the phase boundaries are

$$N_{c,d} = N_i \left[ 1 \mp \sqrt{\pi b \alpha} \frac{R\eta}{Ze} \left( \frac{R}{r_s} \right)^{\frac{3}{4}} \right], \quad (20)$$

$$s_{c,d} = \frac{1}{v_0} \exp \left[ -\frac{r_s Z^2 e^2}{2k_B T D R^2} \left( 1 \pm 2\sqrt{\pi b \alpha} \frac{R\eta}{Ze} \left( \frac{R}{r_s} \right)^{\frac{3}{4}} \right) \right]. \quad (21)$$

The phase diagram is shown in Fig. 4b.

Besides the general properties of the phase diagram discussed in Sec. II, several comments should be made. First, in Eq. (15), since  $R\eta \ll Ze$  and  $r_s \gg R$ ,  $N_{c,d}$  are very close to  $N_i$ . In Eq. (20), since  $R\eta/Ze \simeq A/R$ , we have

$$N_{c,d} \simeq N_i \left[ 1 \mp \frac{A}{(Rr_s^3)^{1/4}} \right]. \quad (22)$$

Again  $N_{c,d}$  are close to  $N_i$ . In both cases, condition (10) is satisfied. Second, in Eqs. (16) and (21), by similar argument,  $s_{c,d} \ll 1/v_0$ . As  $r_s$  decreases,  $s_d$  decreases and  $s_c$  increases. In Fig. 4, as  $r_s$  decreases, the aggregation domain at small  $p$  shrinks.

It is interesting to notice that there is actually the second mechanism of aggregation in the case of strong screening ( $A \ll r_s \ll R$ ). Instead of the global rearrangement of polymer segments on the surface of spheres, the monovalent salt can condense in the disk-like region to make it neutral. This mechanism is competitive because the monovalent salt can only neutralize the disk-like region instead of the whole stripe-like region in Fig. 8. Below we calculate the phase diagram for the second mechanism and compare them with that of the first one.

To get the phase diagram, we start from the two equilibrium conditions which must be satisfied when the aggregated state and the dispersed state are in equilibrium.

$$\mu_c + \frac{ZeQ^*}{C} = k_B T \ln[(s - pN)v_0], \quad (23)$$

$$\epsilon - \frac{\beta Q^{*2}}{2C} = \frac{\beta |Q^*|}{e} k_B T \ln \frac{n}{n_s}, \quad (24)$$

where  $n$  and  $n_s$  are the concentration of the monovalent ions in the bulk and on the surface of the disk-like region. These two equations are analogous to Eqs. (2) and (3). Eq. (23) is the equilibrium condition for spherical Z-ions. The left hand side is the free energy gain when one Z-ion condenses into a macroion-Z-ions complex. The right hand side is the free energy loss of the same process due to the entropy of Z-ions. Eq. (24) is the equilibrium condition for macroion-Z-ions complexes. The left hand side is the free energy gain of the system when one macroion-Z-ions complex aggregate. The first term is the additional correlation energy gain due to aggregation, the second term is the reduction of self-energy since the region is almost neutral in the aggregate. The right hand side is the free energy loss, due to the entropy loss of monovalent counter ions with number  $\beta |Q^*|/e$ . Here since the concentration  $n$  is large for a small  $r_s$ , we assume that the entropy of monovalent salt is a constant in the bulk. Also similarly to the theory in Sec. II, we can assume that the correlation energy  $\mu_c$  is not changed by condensation of monovalent salt in the neutral region. This assumption will be justified later. Obviously,  $\mu_c$ ,  $\epsilon$  and  $C$  are still given by Eqs. (17), (13) and (19). While  $\beta$  is now

$$\beta = b \frac{\pi W_s^2}{4\pi R^2} = \frac{br_s}{4R}. \quad (25)$$

The entropy of the monovalent salt can be roughly estimated as

$$k_B T \ln \frac{n}{n_s} = -k_B T \ln \frac{r_s^2}{a^2} = -\frac{2e\eta_c}{D} \ln \frac{r_s}{a}, \quad (26)$$

where  $k_B T \equiv e^2/Dl_B$ ,  $l_B \simeq 0.7$  nm being Bjerrum length, and for convenience, notation  $\eta_c = e/l_B$  is introduced. Now we can find out the critical  $Q^*$  at which the aggregate forms or dissolves. Solving Eq. (24), we get

$$Q_{c,d}^* = \mp \frac{\pi\alpha}{\ln(r_s/a)} \frac{R^2\eta^2}{r_s\eta_c} N_i, \quad (27)$$

$$N_{c,d} = N_i \left( 1 \mp \frac{\pi\alpha}{\ln(r_s/a)} \frac{R^2\eta^2}{r_s\eta_c Z e} \right). \quad (28)$$

In this procedure we have ignored the  $Q^{*2}$  term in Eq. (24) since it is much smaller. One can easily check that Eq. (27) is consistent with this approximation. Then we can use Eq. (17) to find out the boundaries of the aggregation domain. We have

$$s_{c,d}(p) = s_{c,d} + pN_{c,d}, \quad (29)$$

where

$$\begin{aligned} s_{c,d} &= \frac{1}{v_0} \exp \left[ \frac{1}{k_B T} \left( \frac{ZeQ_{c,d}^*}{C} - |\mu_c| \right) \right] \\ &= \frac{1}{v_0} \exp \left[ -\frac{r_s Z^2 e^2}{2k_B T D R^2} \left( 1 \pm \frac{2\pi\alpha}{\ln(r_s/a)} \frac{R^2\eta^2}{r_s\eta_c Z e} \right) \right]. \end{aligned} \quad (30)$$

A special nature of this mechanism is that there is no partial aggregation domain in the phase diagram. In the first mechanism, we have the partial aggregation domain because upon aggregating, the density of polymer turns on the surface of spheres is changed and so does the number of spheres in a complex. Thus the free energy given by Eq. (1) can take the minimum value with  $0 < x < 1$ . In the present mechanism, the aggregation is induced by the condensation of monovalent ions. The density of polymer turns and the number of spheres in a complex does not change upon aggregating. The free energy can take the minimum value only at  $x = 0$  or  $x = 1$ . There is no partial aggregation domain at all.

Comparing Eqs. (20) and (21) with Eqs. (28) and (30), we see that the difference between results of two mechanisms is not large and depends on the specific values of parameters such as  $R$ ,  $r_s$  and  $\eta$ . If we take  $\eta = \eta_c$ ,  $R = 100\text{\AA}$ ,  $r_s = 10\text{\AA}$ ,  $b = 6$ ,  $\alpha = \ln 2$ , the first mechanism wins.

An artificial chromatin system in the presence of monovalent salt is studied in experiments<sup>15</sup>, where the partial aggregation domain is not observed. This is qualitatively consistent with our theory that the relative size of the partial aggregation domain is small due to screening effect of monovalent salt.

To conclude this section, let us make a final comment about the role of Manning condensation. In this section we are really considering the case when the linear charge density of the polymer  $\eta < \eta_c$ . As is well known, at  $\eta > \eta_c$  (for example, for DNA  $\eta = 4.2\eta_c$ ),  $\eta$  should be renormalized due to Manning condensation. This renormalization of the linear charge density and its consequence on the phase diagram is considered in Ref. 11.

#### IV. RIGID SPHERICAL AND CYLINDRICAL MACROIONS

In this section, we consider systems with rigid spherical or cylindrical macroions and much smaller spherical Z-ions (Figs. 2 and 3). The input parameters  $\mu_c$ ,  $\epsilon$ ,  $C$  and  $\beta$  are calculated microscopically, and the phase diagrams are obtained. We show that  $s_d$  in these two systems is very large, correspondingly the aggregation domain at small  $p$  is very wide in the phase diagram (Fig. 4). The neutral area ratio,  $\beta$  is smaller in the spherical macroion system than in the cylindrical macroion system. As a result,  $s_d$  is smaller in the former case.

First let us consider spherical macroion systems,  $r_s \gg R$ . In this case, each macroion carry  $N_i$  Z-ions in the aggregate and  $\beta = 1$ . Since Z-ions repel each other to form 2D Wigner crystal on the surface of a macroion in the first order approximation, the correlation chemical potential  $\mu_c$  is approximately<sup>16</sup>

$$\mu_c = -\frac{1.6Z^2e^2}{Dr}, \quad (31)$$

where  $r$  is the radius of the Wigner-Seitz cell when a macroion is neutralized by Z-ions. To calculate  $\epsilon$ , we first notice that only Z-ions in the contact region gain the additional correlation energy (see Fig. 5, where the distance  $A$  between two polymer turns corresponds to  $2r$  between two Z-ions in the present case). Similar to the last section, in the present case,  $W \simeq \sqrt{Rr}$ . Bearing in mind that the aggregate is neutral, the number of Z-ions in this region is

$$N_i \frac{\pi W^2}{4\pi R^2} = \frac{\sqrt{N_i}}{2}, \quad (32)$$

where relation  $N_i = 4\pi R^2/\pi r^2$  has been used. If each macroion has  $b$  nearest neighbors in the aggregate ( $b = 12$  for dense packing), the total correlation energy gain of one macroion in the aggregate is

$$\epsilon = \frac{b}{2} \sqrt{N_i} \alpha \mu_c = -0.4b\alpha \frac{ZeQ}{DR}. \quad (33)$$

Here we assume each Z-ion gains correlational energy  $\alpha\mu_c$ . Since the surface density of Z-ions is doubled in the contact region, the radius of the WC cell becomes  $r/\sqrt{2}$  and the correlation energy becomes  $\sqrt{2}\mu_c$ . So  $\alpha \simeq 0.4$ . Finally, for a spherical macroion with Z-ions whose size is negligible, the capacitance is

$$C = DR. \quad (34)$$



Using Eqs. (4) and (6), the characteristic quantities of the phase diagram are given by

$$N_{c,d} = N_i \left( 1 \mp \sqrt{0.2b\alpha} \frac{r}{R} \right), \quad (35)$$

$$s_{c,d} = \frac{1}{v_0} \exp \left[ -\frac{1.6Z^2e^2}{k_B T D r} \left( 1 \pm \sqrt{\frac{b\alpha}{0.8}} \right) \right]. \quad (36)$$

Now let us consider the screening effect of monovalent salt when  $r \ll r_s \ll R$ . First of all, since  $r_s \gg r$ , the short range correlation is not changed by screening,  $\mu_c$  and  $\epsilon$  are still given by Eqs. (31) and (33). The reason for this is the contact region where the additional correlational energy is gained is much smaller than the neutral region (see Sec. II). Using the similar way of estimating  $W$ , for the radius of the neutral region,  $W_s$ , we get  $W_s \simeq \sqrt{Rr_s}$  (see Fig. 7). From this, the area ratio  $\beta$  is

$$\beta = b \frac{\pi W_s^2}{4\pi R^2} = \frac{br_s}{4R}. \quad (37)$$

Finally, the capacitance now is

$$C = \frac{DR^2}{r_s}. \quad (38)$$

Using Eqs. (4) and (6), the specifications of the phase boundaries are

$$N_{c,d} = N_i \left( 1 \mp \sqrt{0.8\alpha} \frac{r}{r_s} \right), \quad (39)$$

$$s_{c,d} = \frac{1}{v_0} \exp \left[ -\frac{1.6Z^2e^2}{k_B T D r} \left( 1 \pm \sqrt{\frac{\alpha}{0.2}} \right) \right]. \quad (40)$$

We then consider cylindrical macroions (Fig. 3) with linear charge density  $-\eta$  ( $Q = L\eta$ ). Before discussing the phase diagram, we specify some geometrical properties of the cylinder. First there is an important ratio,

$$\frac{r}{R} = \sqrt{\frac{2L}{N_i R}} = \sqrt{\frac{2Ze}{\eta R}}, \quad (41)$$

where the relation  $N_i \pi r^2 = 2\pi RL$  has been used. In most practical cases,  $r \ll R$ . It is easy to check that this is the condition that 2D WC of Z-ions is formed on the surface of macroions<sup>14</sup>. Second, we always have  $r_s < L$  for a long cylinder. Consequently below we only focus on two cases corresponding to  $R \ll r_s \ll L$  and  $r \ll r_s \ll R$ . Third, inequality  $R \ll L$  leads to certain preference when a macroion aggregates. To gain more contact area and therefore more correlation energy, all cylinders in the aggregate are parallel to each other.

Now let us consider the case when  $R \ll r_s \ll L$ . It is easy to see that the aggregate should be neutral, i.e.,  $\beta = 1$ . Obviously, the chemical potential  $\mu_c$  is still given by Eq. (31). However,  $\epsilon$  is not the same as the spherical macroion case because the area of the contact region is

much larger. It is not a disk, but a stripe with area  $2WL$ . The number of Z-ions in the contact region is

$$N_i \frac{2WL}{2\pi RL} = \frac{1}{\pi} N_i \sqrt{\frac{r}{R}}. \quad (42)$$

For a macroion with  $b$  nearest neighbors ( $b = 6$  for dense packing), the additional correlation energy per macroion is

$$\epsilon = \frac{b\alpha}{\pi} N_i \mu_c \sqrt{\frac{r}{R}}. \quad (43)$$

And the capacitance is

$$C = \frac{DL}{2 \ln(r_s/R)}. \quad (44)$$

Using Eqs. (4) and (6), we have

$$N_{c,d} = N_i \left[ 1 \mp \sqrt{\frac{0.8b\alpha}{\pi \ln(r_s/R)}} \left( \frac{r}{R} \right)^{\frac{3}{4}} \right], \quad (45)$$

$$s_{c,d} = \frac{1}{v_0} \exp \left[ -\frac{1.6Z^2e^2}{k_B T D r} \left( 1 \pm \sqrt{\frac{b\alpha}{0.2\pi}} \ln \frac{r_s}{R} \left( \frac{R}{r} \right)^{\frac{1}{4}} \right) \right]. \quad (46)$$

Now we consider the case when  $r \ll r_s \ll R$ . Instead of a neutral aggregate, we only require a neutral region which is a stripe-like region in the present case. It is easy to see that both  $\mu_c$  and  $\epsilon$  are not changed by screening. The fraction of neutral area is

$$\beta = b \frac{2W_s L}{2\pi RL} = \frac{b}{\pi} \sqrt{\frac{r_s}{R}}, \quad (47)$$

while the capacitance

$$C = \frac{DRL}{2r_s}. \quad (48)$$

The characteristic quantities of aggregation are obtained using Eqs. (4) and (6):

$$N_{c,d} = N_i \left[ 1 \mp \sqrt{0.8\alpha} \left( \frac{r}{r_s} \right)^{\frac{3}{4}} \right], \quad (49)$$

$$s_{c,d} = \frac{1}{v_0} \exp \left[ -\frac{1.6Z^2e^2}{k_B T D r} \left( 1 \pm \sqrt{\frac{\alpha}{0.2}} \left( \frac{r_s}{r} \right)^{\frac{1}{4}} \right) \right]. \quad (50)$$

Besides the general properties of the phase diagram discussed in Sec. II, several comments should be made to the results in this section. First, from the expressions of  $N_{c,d}$ , it is easy to check that in all cases  $N_{c,d}$  are close to  $N_i$  and condition (10) is satisfied. Second, from the expressions of  $s_d$  in this section,  $s_d$  ( $s_c$ ) is larger (smaller) in the case of cylindrical macroions than in the case of spherical macroions. Third, we see that  $s_d$  is in the order of  $1/v_0$  (in spherical macroion case) or even larger than

$1/v_0$  (in cylindrical macroion case). Consequently, one may conclude that the aggregate never dissolve at large  $s$ . Actually, this is not true. When  $s$  becomes so large that the distance between Z-ions in the bulk is equal to  $r_s$ , the repulsion between free Z-ions can not be ignored and our theory is invalid. At such a large concentration, Z-ions are correlated not only on the surface of macroions but also in the solution and the aggregation does not happen. What we can conclude is that for systems discussed in this section, the aggregate dissolves only at certain very large  $s$ . Mathematically,  $s_d$  is very large so that  $\ln(s_d v_0) \leq \ln(s_d/s_c)$ . Correspondingly, the aggregation domain in Fig. 4 at  $s > s_i$  is very wide. Thus the systems discussed in this section are very different from the artificial chromatin system in which  $s_d$  is exponentially small.

Finally, let us discuss applications of our theory. In the case of spherical macroion system, several Monte Carlo simulations have been done recently<sup>17,18</sup>. It is reported that around the isoelectric line  $s_i = pN_i$  (dotted line in Fig. 4), all macroions aggregate. Also there is a certain asymmetry between the two sides of this line. The aggregation domain looks wider in the upper side of this line<sup>18</sup>, which agrees with our theory.

The results of cylindrical macroion system can be qualitatively applied to the DNA-spermine system<sup>4,5,6,7</sup> in which long DNA are considered as rigid cylinder and short spermines as small Z-ions. In experiments, a very wide aggregation domain at small  $p$  ( $\log(s_d/s_c) \simeq 4$ ) is observed, which again agrees with our theory.

## V. CONCLUSION

In conclusion, we discuss kinetic aspects of the aggregation problem. Above we discussed only equilibrium phase diagrams. It is known that some solutions of oppositely charged colloids slowly approach their equilibrium (aggregated) states<sup>8,9,10</sup>. To talk about kinetics, we should first specify the initial conditions of the system. Below we assume that all solutions are prepared by putting necessary amounts of two colloids into water solution at the same time. Since macroion-Z-ions complexes are formed relatively fast, the kinetics we are interested in starts from aggregation of two complexes<sup>21</sup>. As we know, away from the dashed line on Fig. 4, complexes are likely charged and repel each other. As a result, the Coulomb barrier slows down their aggregation. This leads to slow aggregation in the cases of spherical (Fig.2) and cylindrical complexes (Fig.3)<sup>21</sup>. On the other hand, for the self-aggregation of a long artificial chromatin (Fig. 1), the role of kinetics may not be as important because spheres in the same complex are already close to each other and barriers can be smaller.

In the case when the slow kinetics is observed, it is sometimes useful to discuss the “effective phase diagram” of the system at certain time  $t$ , when the thermal equilibrium has not been reached. The aggregation domain

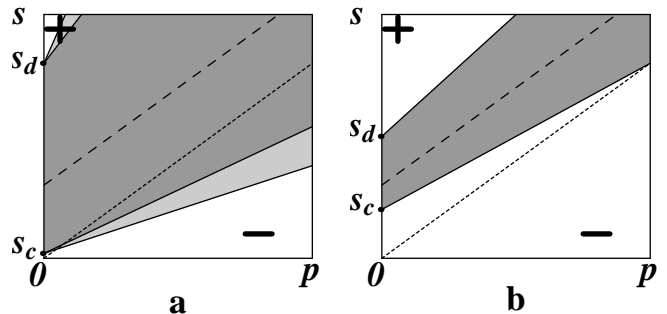


FIG. 9: **a**: equilibrium phase diagram of spherical macroion system with monovalent salt. **b**: effective phase diagram of the same system at time  $t$  when the equilibrium state has not been reached.  $s_{c,d}$  in plot **b** are functions of time. All other labels have the same meaning as in Fig. 4.

of such a phase diagram is defined as all compositions for which the average size of aggregates reaches certain critical value during the time  $t$ . As we know, near the dashed line on Fig. 4, all macroion-Z-ions complexes are neutral so that there is no Coulomb barrier and the kinetics is very fast. On the other hand, when one moves away from the dashed line, the absolute value of the net charge of macroion-Z-ions complexes grows and so does the Coulomb barrier. The larger the net charge, the higher the barrier, the slower the kinetics. As a result, at time  $t$ , only solutions located in some vicinity of the dashed line can reach the stage where the average size of aggregates is above the critical value. As  $t$  increases, more solutions reaches the stage and the effective aggregation domain grows. At  $t \rightarrow \infty$ , it becomes identical with the equilibrium aggregation domain. As an illustration, we show the effective phase diagram of a spherical macroion system (Fig. 2) with monovalent salt at certain time  $t$  in Fig. 9b. The equilibrium phase diagram of the same system is shown in Fig. 9a for a comparison. A quantitative theory of the growth of the effective aggregation domain will be addressed in a future paper.

## Acknowledgments

The authors are grateful to S. Grigoryev, V. Lobaskin, T.T. Nguyen, E. Raspaud and J. H. van Zanten for useful discussions. This work is supported by NSF No. DMR-9985785.

<sup>1</sup> B. Alberts, A. Johnson, J. Lewis, M. Raff, K. Roberts, and P. Walter, *Molecular Biology of the Cell* (Galland, New

York, 2002).

- <sup>2</sup> J. Widom, *J. Mol. Biol.*, **190**, 411 (1986).
- <sup>3</sup> V. A. Bloomfield, C. Ma, and P. G. Arscott, *ACS Symp. Ser.*, **548**, 185 (1994).
- <sup>4</sup> J. Pelta, F. Livolant, and J.-L. Sikorav, *J. Biol. Chem.*, **271**, 5656 (1996).
- <sup>5</sup> E. Raspaud, M. Olvera de la Cruz, J.-L. Sikorav, and F. Livolant, *Biophysical Journal*, **74**, 381 (1998).
- <sup>6</sup> E. Raspaud, I. Chaperon, A. Leforestier, and F. Livolant, *Biophysical Journal*, **77**, 1547 (1999).
- <sup>7</sup> M. Saminathan, T. Antony, A. Shirahata, L. H. Sigal, T. Thomas, and T. J. Thomas, *Biochemistry*, **38**, 3821 (1999).
- <sup>8</sup> E. Lai and J. H. van Zanten, *Biophysical Journal*, **80**, 864 (2001).
- <sup>9</sup> E. Lai and J. H. van Zanten, *Journal of Controlled Release*, **82**, 149 (2002).
- <sup>10</sup> H. W. Walker and S. B. Grant, *Colloids and Surfaces A*, **119**, 229 (1996) and reference therein.
- <sup>11</sup> T. T. Nguyen and B. I. Shklovskii, *J. Chem. Phys.*, **115**, 7298 (2001).
- <sup>12</sup> C. Tse, T. Sera, A. P. Wolffe, and J. C. Hansen, *Mol. Cel. biology*, **18**, 4629 (1998).
- <sup>13</sup> The definition of  $\epsilon$  is different from Ref.11. There  $\epsilon$  is used to define the additional correlation energy per Z-ion in the aggregate. The connection is  $\epsilon = N_i \epsilon$ . The definition used here is more convenient because for systems like Fig. 2 and Fig. 3 not all Z-ions in the aggregate can gain the additional correlation energy.
- <sup>14</sup> B.I. Shklovskii, *Phys. Rev. Lett.*, **82**, 3268 (1999).
- <sup>15</sup> K. Keren, Y. Soen, G. Ben Yoseph, R. Gilad, E. Braun, U. Sivan, and Y. Talmon, *Phys. Rev. Lett.*, **89**, 088103 (2002).
- <sup>16</sup> A. Yu. Grosberg, T. T. Nguyen, and B. I. Shklovskii, *Rev. Mon. Phys.*, **74**, 329 (2002).
- <sup>17</sup> P. Linse and V. Lobaskin, *Phys. Rev. Lett.*, **83**, 4208 (1999).
- <sup>18</sup> V. Lobaskin and K. Qamhieh, *cond-mat/0212182*.
- <sup>19</sup> T.T. Nguyen, I. Rouzina, and B. I. Shklovskii, *J. Chem. Phys.*, **112**, 2562 (2000).
- <sup>20</sup> T.T. Nguyen and B. I. Shklovskii, *J. Chem. Phys.*, **114**, 5905 (2001).
- <sup>21</sup> T.T. Nguyen and B. I. Shklovskii, *Phys. Rev. E*, **65**, 031409-1 (2002).